Towards semi-automated image analysis

For local bubble behavior

Emilie Overgaard Willer[a], Maximilian Siska[b], Juliet J. Victoria[a], Eric von Lieres[b,c], & John M. Woodley[a]

[a]Department of Chemical and Biochemical Engineering, Technical University of Denmark, 2800 Kgs. Lyngby, Denmark
[b]Institute of Bio- and Geosciences, Forschungszentrum Jülich GmbH, 52428 Jülich, Germany
[c]Computational Systems Biotechnology, RWTH Aachen University, 52074 Aachen, Germany

eoje@kt.dtu.dk

Introduction

Many bioprocesses depend on oxygen, and its low aqueous solubility makes bubble behavior crucial to understand. This behavior is affected by factors such as flow rate, power input, and viscosity. Numerous correlations for oxygen mass transfer and bubble size have been established over decades. However, these models typically rely on reactor-averaged measures and therefore fail to provide insights into local hydrodynamic gradients. Bubble size significantly influences oxygen mass transfer k_La, an essential parameter for oxygen dependent bioprocess. Therefore, obtaining the optimum bubble size possible is essential. Dividing the parameter k_La into liquid film diffusion, k_L, and the specific interfacial area, a, can help understand the bubble size effect on the system.

O_2

O_2

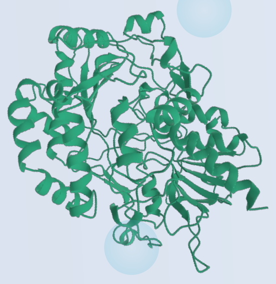

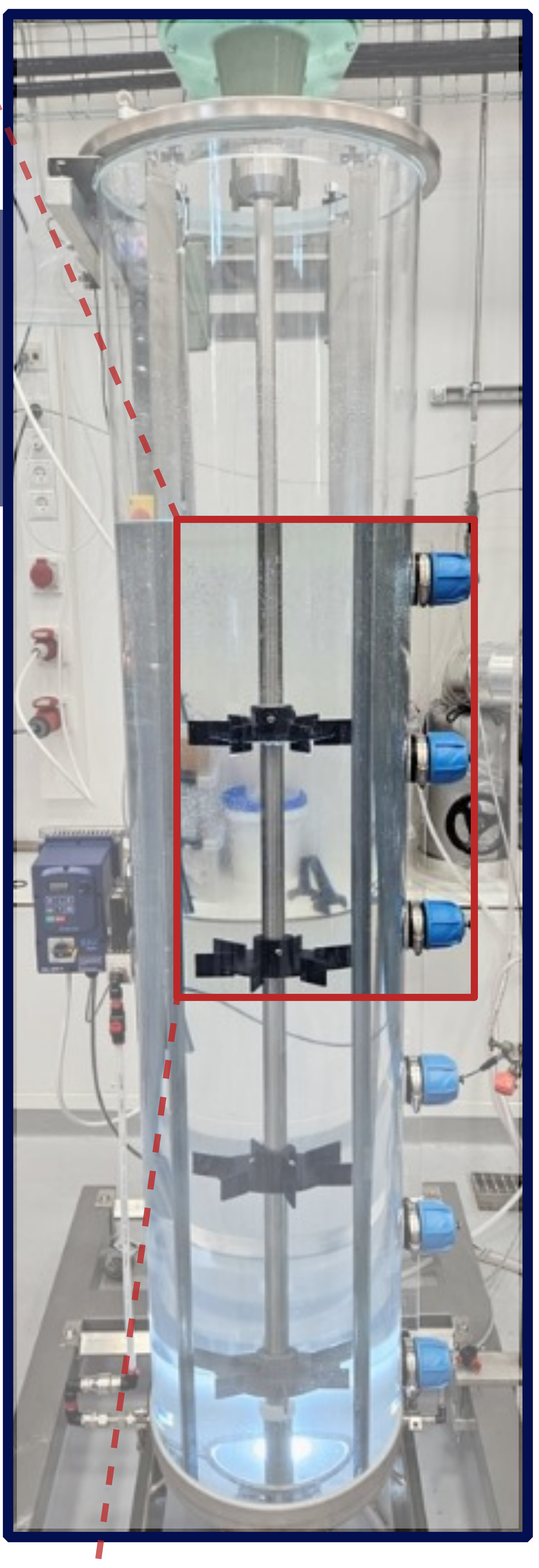

Shadowscope: Raw images

The inline shadowscope enables local gas bubble size examination.
The endoscope consists of a ShadowStrobe LED, providing LED back illumination and a lens performing long-distance telecentric optic connected to a high-speed camera. The endoscope´s field of view is 146 mm by 117 mm by 40 mm (width by height by depth). For the experimental setup, 1000 images were captured with a 10 Hz trigger rate (10 frames per second).

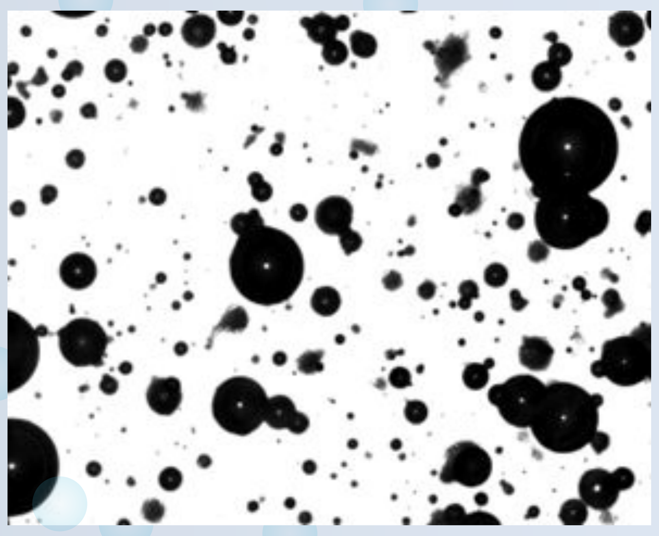

Image processing

Bubbles are detected based on a pixel-level mask, by the use of a manually trained YOLOv11x segmentation model. From which their shape is classified and their three-dimension geometry is reconstructed.
The model distinguishes between noise, such as impurities and artifacts from the gas bubbles.

- Spherical x/y ratio <10% of unity (Green)
- non-spherical treated as asymmetric ellipsoids (Red)

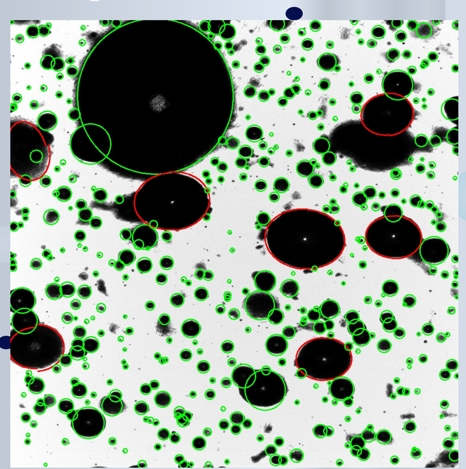

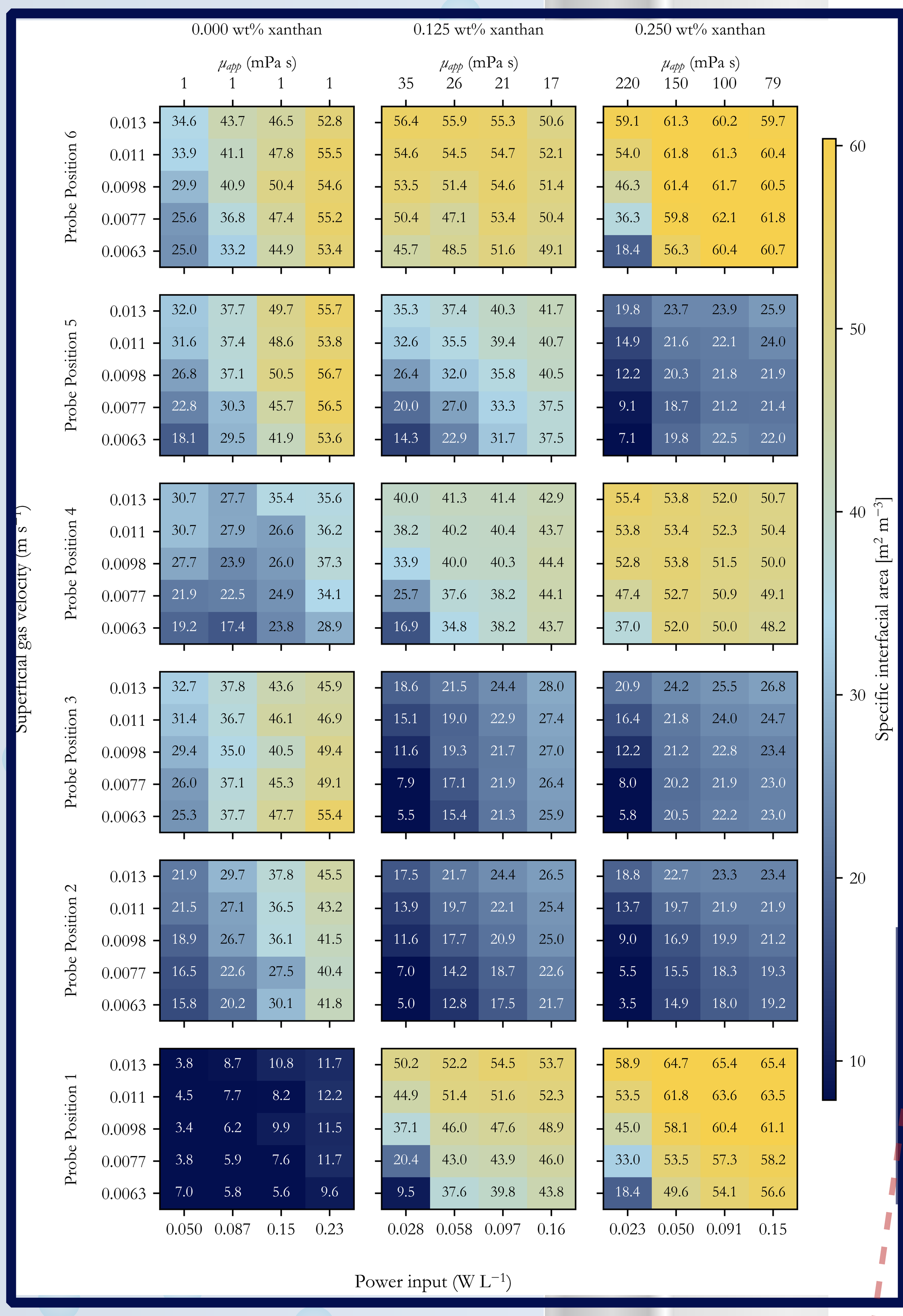

Data processing

Based on the pixel mask, the bubble size and shape is defined. Providing a gas bubble size distribution.
From the three-dimensional geometry construction, the individual gas bubbles volume and specific interfacial area are defined.
Which can be used for providing information on local gas holdup.
Experiments were conducted in a 185L working volume pilot scale reactor. Testing 5 aeration rates (45, 55, 70, 80, & 90 L/min) 4 stirrer speeds (75, 100, 125, & 150 RPM), and 3 viscosities (0.000, 0.125, 0.250 wt% of xanthan gum) in a electrolyte solution (0.05M $MgSO_4$).
Example of Bubble size distribution across viscosity for 100 rpm and 70 L/min

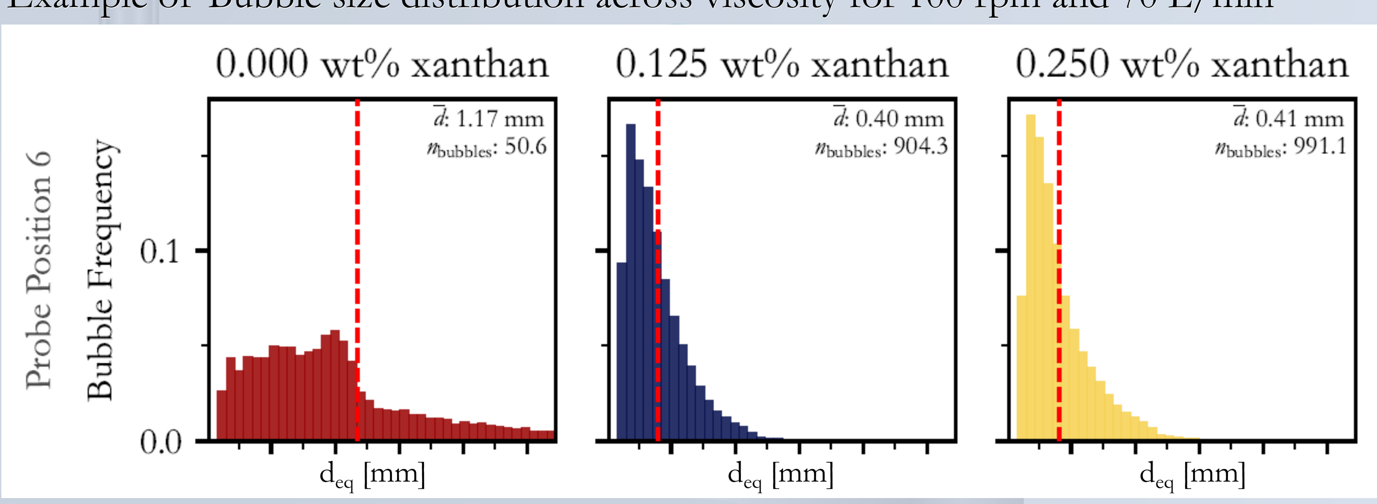

Key Findings:

- High a at position 6 due to gas entrainment & foam formation stabilizing gas bubbles
- Stagnant zones around position 2, 3, & 5
- Bubble count increasing with viscosity
- Viscous forces dominating gas bubble shape

Bubble size distribution
↓
interfacial area
↓
k_L modeling
↓
Local k_La
↓
Process modeling
↓
Scale-up

This project has received funding from the European Research Council (ERC) under the European Union´s Horizon 2020 research and innovation programme. (Grant agreement No. 101021024)